JOURNAL OF THERMOPHYSICS AND HEAT TRANSFER
Vol. 16, No. 3, July–September 2002

Exact Solution for Nonlinear Thermal Diffusion and Its Use for Verification

Robert L. McMasters* and Zhengfang Zhou†
Michigan State University, East Lansing, Michigan 48824
Kevin J. Dowding‡
Sandia National Laboratories, Albuquerque, New Mexico 87185
and
Craig Somerton§ and James V. Beck¶
Michigan State University, East Lansing, Michigan 48824

An analytical solution is provided to the nonlinear diffusion equation, with the thermal conductivity given as a linear function of temperature. The derivation of the solution, and implications of it, are presented. The boundary and initial conditions associated with the solution provide applicability to specific cases. The solution is useful for verifying numerical (computer) solutions to thermal diffusion with temperature-dependent thermal conductivity. The (nonlinear) analytical solution is compared to a numerical solution from a finite element code to verify the accuracy of the code and to establish the order of convergence for the spatial discretization error.

Nomenclature

C	=	error constant
c	=	volumetric heat capacity, J/m^3 · K
$\|e\|_m$	=	general error norm, K
Fo_h	=	mesh Fourier number (dimensionless)
f	=	time-dependent separation variable (dimensionless)
g	=	spatial dependent separation variable (dimensionless)
H_1	=	error seminorm, K/m
h	=	characteristic mesh size, m
h_c	=	convection coefficient, W/m^2 · K
k	=	thermal conductivity, W/m · K
k_0	=	thermal conductivity at $T = 0$, W/m · K
k_1	=	thermal conductivity sensitivity to temperature, K^{-1}
L_2	=	error norm, K
L_∞	=	error norm, K
p	=	error exponent
T	=	temperature, K
t	=	time, s
w	=	transformation variable for temperature (dimensionless)
x	=	spatial variable, m
β	=	spatial shifting constant (dimensionless)
γ	=	time shifting constant (dimensionless)
θ	=	temperature (dimensionless)
θ_∞	=	ambient temperature (dimensionless)
λ	=	separation of variables constant (dimensionless)

Superscript

$+$	=	dimensionless variable

Received 27 August 2001; revision received 28 October 2001; accepted for publication 16 January 2002.

*Instructor, Department of Mechanical Engineering; mcmaste7@msu.edu.
†Professor, Department of Mathematics.
‡Senior Member of Technical Staff, Validation and Uncertainty, Quantification Processes Department 9133.
§Associate Professor, Department of Mechanical Engineering.
¶Professor Emeritus, Department of Mechanical Engineering.

I. Introduction

TWO related subjects are addressed in this paper. The first subject is a procedure to develop an analytical solution to the mathematical equation of nonlinear thermal diffusion. The nonlinearity results from thermal conductivity varying linearly with temperature. The second subject is the verification of a numerical computer code. When the analytical solution is used, the correctness and accuracy of a computer code to simulate numerically nonlinear thermal diffusion is assessed.

The solution to the linear diffusion equation for heat conduction has long been accomplished using separation of variables, as pioneered by Sturm and Liouville.[1] Subsequent to the introduction of the method of separation of variables, the method of Green's functions has been used to solve a variety of specific cases of linear heat conduction problems. This method has been advanced by Beck et. al.[2] and has been used in solving the diffusion equation for heat conduction under a wide variety of boundary and initial conditions. Temperature-dependent thermal conductivity and volumetric heat capacity have been dealt with using the Kirchhoff transformation (see Ref. 3), where the temperature dependence of conductivity and volumetric heat capacity are identical to one another, yielding a constant diffusivity. Becker[4] examined similarity solutions of the nonlinear heat conduction problem, involving a local heat pulse, and found a solution analogous to a Green's function for the linear problem.

In contrast to the linear-based methods just discussed the present research provides an algebraic form of the solution of the nonlinear thermal diffusion equation when the thermal conductivity varies linearly with temperature and volumetric heat capacity is constant. For many materials, the thermal parameters in the diffusion equation are strong functions of temperature.[5] In such cases, the conventional linear solution methods are no longer applicable.

This paper provides the derivation of an exact analytical solution for a nonlinear thermal diffusion problem. The analytical solution provides insight into anomalous behavior inherent in nonlinear equations. The boundary and initial conditions for the solution are determined from the solution itself. The primary use of the solution is intended to be for verification of numerical computer codes, which can treat arbitrary boundary and initial conditions. The solution is well suited for verification because it has a simple analytical form and it can be precisely and unambiguously evaluated.

Greater reliance on the use of computational physical simulation in the engineering design process has increased our need to quantify

the accuracy of computational simulations. There are broadly two classifications of accuracy. The first classification addresses whether the instantiation of the mathematical physical models, including solution algorithms, are accurate; this is verification. The second classification addresses whether computational models are an accurate representation of physical processes and involves experimentation; this is validation. A succinct description[6] is that verification determines whether we are solving the equations right, whereas validation determines whether we are solving the right equations. Verification needs to be done before addressing validation. Verification and validation as applied to understanding the accuracy of the physical (computer) simulations are a growing area of study (see Refs. 6 and 7). Verification is addressed in this paper.

The verification process compares a computer program's numerical solution to a solution obtained independently to assess the accuracy of the program. In this case, we compare the numerical solution to an analytical solution. Because numerical solutions depend on a discrete representation, we must address the dependence of the numerical solution on the discretization. Hence, verification should establish that the numerical solution is accurate, that the accuracy improves as the discretization is refined, and that the discretization error decreases at a rate consistent with the theoretical rate of convergence for the numerical method. Having achieved the theoretical convergence rate, we are confident that the computer program is solving the mathematical equations accurately and is free of error.

Verification is an exercise in mathematics to address whether the computer program is accurately solving the mathematical equations. Solutions based on physically realistic problems are not necessarily required. Roach[6] advocates the method of manufactured solutions in which a (analytical) function is arbitrarily selected as the solution. Terms remaining after passing the function through the mathematical differential equation are imposed as volumetric source terms. The method of manufactured solutions typically results in a space-/time-dependent volumetric source term as well as space-/time-dependent boundary and initial conditions. To verify a mathematical differential equation that is not solved with a volumetric source term, the assumed function must be carefully selected (as outlined in this paper). Similarly, for verifying mathematical equations that include boundary and initial conditions of a simple prescribed form, typically constants, additional requirements on the assumed function must be imposed. In this case, analytically solving the mathematical equations may be an avenue for obtaining a solution. To verify the various aspects of the code that discretize the mathematical equation representing the describing differential equation while imposing boundary and initial conditions, a host of solutions (manufactured and exact analytical) are required.

The analytical solution presented in this paper contains a singularity that causes the computed temperature to reach infinity at some point on the time continuum. Provided the numerical and exact solutions are evaluated at a time close enough to the singularity that the solution is not effectively constant in the spatial continuum, the solution is useful for verification. This singularity may help to quantify the limit of a numerical method in terms of its ability to follow the exact solution at the theoretical convergence rate. Moving closer to the singularity and stressing the numerical solution may provide additional insight to the limits of the theoretical characteristics of the numerical approximation. This feature of the anlaytical solution is not studied in this paper.

An outline of the paper is now given. The solution to the nonlinear differential equation for the problem is provided in Sec. II. The application of initial and boundary conditions is discussed in Sec. III. Graphical representations of dimensionless results are presented in Sec. IV. Verification of a numerical solution, through a comparison with the exact solution, is discussed in Sec. V with a summary of results in Sec. VI.

II. Solution

In this paper, the thermal conductivity is assumed a linear function of temperature, expressed as

$$k = k_0(1 + k_1 T) \tag{1}$$

where k is the thermal conductivity at the temperature T and the product k_0k_1 represents the slope of thermal conductivity variation with temperature. The differential equation for heat conduction, using Eq. (1) for thermal conductivity, is

$$c\frac{\partial T}{\partial t} = k_0\frac{\partial}{\partial x}\left[(1 + k_1 T)\frac{\partial T}{\partial x}\right] \tag{2}$$

When the transformation $w = 1 + k_1 T$ is used, the partial derivatives of w can be written as

$$\frac{\partial w}{\partial t} = k_1\frac{\partial T}{\partial t}, \qquad \frac{\partial w}{\partial x} = k_1\frac{\partial T}{\partial x} \tag{3}$$

Substituting these derivatives into Eq. (2) gives

$$\frac{c}{k_1}\frac{\partial w}{\partial t} = \frac{k_0}{k_1}\frac{\partial}{\partial x}\left[w\frac{\partial w}{\partial x}\right] \quad \text{or} \quad c\frac{\partial w}{\partial t} = \frac{k_0}{2}\frac{\partial^2(w^2)}{\partial x^2} \tag{4}$$

With use of the separation of variables principle, let $w(x, t) = f(t)g(x)$, and substitute this into Eq. (4) to get

$$cf'g = (k_0/2)f^2(g^2)'' \tag{5}$$

where $f' \equiv \mathrm{d}f/\mathrm{d}t$ and $g'' \equiv \mathrm{d}^2g/\mathrm{d}x^2$. Dividing both sides of Eq. (5) by f^2g, we have

$$cf'/f^2 = k_0(g^2)''\big/2g = \lambda \tag{6}$$

where λ is a constant due to the independence of f and g. Examining the time-dependent portion of the solution, we have

$$f'/f^2 = \lambda/c \quad \text{or} \quad (1/f)' = -\lambda/c \tag{7}$$

Integrating both sides gives

$$1/f = \lambda(\gamma - t/c) \quad \text{or} \quad f = 1/[\lambda(\gamma - t/c)] \tag{8}$$

where γ is a constant of integration.

From the x-dependent portion of Eq. (6), we have

$$k_0(g^2)''\big/2g = \lambda \quad \text{or} \quad 2k_0(g^2)'(g^2)'' = 4(g^2)'g\lambda \tag{9}$$

when both sides are multiplied by $4g(g^2)'$. Rearranging each side gives

$$k_0\{[(g^2)']^2\}' = \tfrac{8}{3}(g^3)'\lambda \tag{10}$$

which can be directly integrated to obtain

$$k_0[(g^2)']^2 = \tfrac{8}{3}g^3\lambda \tag{11}$$

Notice that there is some loss of generality in Eq. (11). The constant of integration is taken as zero for convenience to continue with the derivation. Expanding the derivative on the left-hand side yields

$$4k_0g^2(g')^2 = \tfrac{8}{3}g^3\lambda \tag{12}$$

and dividing by $4g^2$ gives

$$k_0(g')^2 = \tfrac{2}{3}g\lambda \tag{13}$$

which produces

$$g' = \sqrt{2\lambda g/3k_0} \quad \text{or} \quad (\sqrt{g})' = \sqrt{\lambda/6k_0} \tag{14}$$

Integrating once again gives

$$\sqrt{g} = \sqrt{(\lambda/6k_0)}(x + \beta) \quad \text{or} \quad g = (\lambda/6k_0)(x + \beta)^2 \tag{15}$$

where β is a constant of integration. Recalling the original definition of the separation of variables as $w(x, t) = f(t)g(x)$ and combining the time and space solutions [Eq. (8) and Eq. (15)] gives

$$w(x,t) = \frac{(x+\beta)^2}{6k_0(\gamma - t/c)} \tag{16}$$

The separation constant λ in Eq. (6) cancels when the time and space solutions are multiplied. The remaining constants, β and γ, are arbitrary and can be redefined as dimensionless quantities. An equivalent expression for $w(x,t)$ using dimensionless β and γ (for convenience the same symbols are used) is

$$w(x,t) = \frac{(x/L+\beta)^2}{6\left(\gamma - k_0 t/L^2 c\right)} \tag{17}$$

Substituting this equation into the original transformation, $w = 1 + k_1 T$, gives the temperature distribution

$$T(x,t) = \frac{1}{k_1}\left[\frac{(x/L+\beta)^2}{6(\gamma - (k_0/c)t/L^2)} - 1\right] \tag{18}$$

Note that this solution is found without specifying initial or boundary conditions. The nature of the solution is such that it does not lend itself to the application of constant boundary conditions. Rather, the boundary conditions follow a functional form dictated by the solution itself. This is due in part to a loss of generality conceded to by arbitrarily forcing a constant of integration to be zero in Eq. (11) of the derivation. The initial and boundary conditions can only be modified by adjusting β and γ.

The temperature solution in Eq. (18) can also be written in dimensionless form as

$$\theta(x^+,t^+) = \frac{1}{6}\frac{(x^+ + \beta)^2}{(\gamma - t^+)} - 1 \tag{19}$$

where the dimensionless variables are

$$\theta(x^+,t^+) \equiv k_1 T(x,t) \tag{20a}$$

$$x^+ \equiv x/L \tag{20b}$$

$$t^+ \equiv k_0 t/cL^2 \tag{20c}$$

A few general comments are now given regarding this solution. Equation (18) is the solution to nonlinear (transient) thermal diffusion in which thermal conductivity is assumed to be a linear function of temperature and the volumetric heat capacity is considered constant. No boundary or initial conditions have been imposed to obtain the solution. The solution has a simple algebraic form but exhibits nonlinear dependence on time, position, and the thermal properties.

One can view the solution in Eq. (18) as a manufactured solution[6] that exactly satisfies the partial differential equation (PDE) for nonlinear thermal diffusion. The method of manufactured solutions[6] is a process to generate an analytical solution to a PDE by assuming a functional form for the solution, passing the assumed solution through the PDE, and grouping the remaining terms in a volumetric source term. Typically the process results in a complicated (time- and space-dependent) volumetric source term. The functional form in Eq. (18) exactly satisfies the PDE for a nonlinear thermal diffusion problem. The solution outlined in this paper provides guidance on a functional form that satisfies the PDE for nonlinear thermal diffusion as well as mathematical techniques to guide selection/derivation of the assumed functional form when applying the method of manufactured solutions.

The two arbitrary constants, β and γ, serve to translate linearly the spatial and temporal dependence, respectively. For the purpose of verification, the space translating constant β can be set to 0. The temporal constant γ shifts the time at which the solution is singular; specifically, the solution is singular at $\gamma = t^+$.

Based on physical requirements, some additional constraints on the solution are that the thermal conductivity and the volumetric heat capacity must both be positive. The value for volumetric heat capacity is constant and can, therefore, be easily specified as greater than zero. The thermal conductivity, however, is a function of temperature and, therefore, varies with time and position. Substituting Eq. (19) into Eq. (1) gives the functional variation of the thermal conductivity

$$k[T(x^+,t^+)] = \frac{k_0(x^+ + \beta)^2}{6(\gamma - t^+)} \tag{21}$$

To maintain $k > 0$, it is necessary that $(\gamma - t^+)/k_0$ be greater than zero. Therefore, if k_0 is positive, we must have $t^+ < \gamma$, and if k_0 is negative, we must have $t^+ > \gamma$. Another way of expressing the allowable values of time for this equation is $t < cL^2/k_0$. Because γ linearly translates the time t, we can have either $\gamma > 0$ and $k_0 > 0$ or $\gamma < 0$ and $k_0 < 0$. It is more convenient to use the solution for which $\gamma > 0$ and $k_0 > 0$.

III. Initial and Boundary Conditions

The initial temperature distribution is given by

$$\theta(x^+,0) = [(x^+ + \beta)^2/6\gamma] - 1 \tag{22}$$

which is found by substituting $t^+ = 0$ into Eq. (19). This equation is quadratic in x^+ and can be either positive or negative.

Boundary conditions are established by the solution and are found by substituting $x^+ = 0$ and 1 into the solution. The boundary conditions for prescribed temperature are

$$\theta(0,t^+) = \frac{\beta^2}{6(\gamma - t^+)} - 1 \tag{23a}$$

$$\theta(1,t^+) = \frac{(1+\beta)^2}{6(\gamma - t^+)} - 1 \tag{23b}$$

Errors in the numerical solution of the temperature are more sensitive to heat flux boundary conditions than to those of prescribed temperature. The heat flux at any point in the continuum is

$$q^+(x^+,t^+) \equiv -k^+\frac{\partial\theta(x^+,t^+)}{\partial x^+} = -\frac{(x^+ + \beta)^3}{18(\gamma - t^+)^2} \tag{24}$$

where k^+ is dimensionless thermal conductivity, defined as k/k_0. This expression is then evaluated at the boundaries to obtain

$$q^+(0,t^+) = -\frac{\beta^3}{18(\gamma - t^+)^2} \tag{25a}$$

$$q^+(1,t^+) = -\frac{(1+\beta)^3}{18(\gamma - t^+)^2} \tag{25b}$$

Notice that, at $x^+ = 0$, the heat flux is zero for $\beta = 0$. Hence, we have the very unusual case of the same surface being both at a constant temperature [Eq. (23a)] and being insulated [Eq. (25a)] for $\beta = 0$. The explanation for the heat flux being zero for $x^+ = 0$ and $\beta = 0$ is that the thermal conductivity goes to zero for this condition [see Eq. (21)].

The solution can also be used to derive convection and radiation boundary conditions. Consider the convection boundary condition at $x^+ = 1$ with $\beta = 0$. The heat flux boundary at $x^+ = 1$ in dimensionless terms can be written from Eq. (25b) as

$$q^+(1,t^+) = -1/18(\gamma - t^+)^2 = -h_c^+[\theta_\infty - \theta(1,t^+)] \tag{26}$$

Two possibilities now exist. We can prescribe a functional for h_c^+ and solve for $\theta_\infty(h_c^+)$ or, the reverse, prescribe θ_∞ and solve for $h_c^+(\theta_\infty)$. When the former is considered, let h_c^+ be a known function. We can solve for the dimensionless ambient temperature

$$\theta_\infty = 1/18h_c^+(\gamma - t^+)^2 + \theta(1,t^+) = 1/18h_c^+(\gamma - t^+)^2 + 1/6(\gamma - t^+) - 1 \tag{27}$$

For a prescribed functional form of the dimensionless convection coefficient given as

$$h_c^+ = 1/18(\gamma - t^+)^2 \tag{28}$$

the dimensionless ambient temperature in Eq. (27) that satisfies the boundary condition in Eq. (26) is

$$\theta_\infty = 1/6(\gamma - t^+) \tag{29}$$

When the functional form for the convection coefficient and ambient temperature given in Eqs. (28) and (29) is specified, the nonlinear analytical solution in Eq. (19) is applicable; a problem with a convection boundary condition can be verified.

Similarly, we can derive boundary conditions for surface radiation. The radiation boundary condition,

$$q^+ = -\sigma\varepsilon\left[\theta(1,t^+)^4 - \theta_\infty^4\right] = -1/18(\gamma - t^+)^2 \tag{30}$$

can be used to obtain the dimensionless ambient temperature, assuming ε is known, of

$$\theta_\infty = [1/18\varepsilon\sigma(\gamma - t^+)^2 + \theta(1,t^+)]^{\frac{1}{4}}$$

$$= [1/18\varepsilon\sigma(\gamma - t^+)^2 + 1/6(\gamma - t^+) - 1]^{\frac{1}{4}} \tag{31}$$

Similar to the convection boundary condition, we can solve for either $\theta_\infty(\varepsilon)$ or $\varepsilon(\theta_\infty)$ where we assume a functional form for the independent variable.

Consequently, the analytical solution to nonlinear thermal diffusion can be used to verify problems with temperature, heat flux, convection, and radiation boundary conditions. Only solutions with prescribed heat flux on the boundary are studied for verification in this paper.

IV. Graphical Presentation of Dimensionless Results

Figures 1 and 2 are the dimensionless temperature solution as a function of dimensionless time and location with $\beta = 0$; Fig. 1 is for $\gamma = 1$, and Fig. 2 is for $\gamma = 0.01$. The latter produces much larger dimensionless temperatures but the shapes in Figs. 1 and 2 are basically the same because the term with the division by $\gamma - t^+$ is much larger than unity as t^+ approaches γ. The values of the dimensionless temperature for the smaller γ approach 500 at the dimensionless time of 0.0098.

Figure 3 shows the dimensionless temperature as a function of location for three different dimensionless times with $\beta = 0$ and $\gamma = 1$. The times are $t^+ = 0.9$, 0.95, and 0.98. These times are chosen to be near the critical dimensionless time of $t^+ = \gamma = 1$. At the selected times, the gradients in the temperature are large, unlike those for t^+ less than 0.5 (for $\gamma = 1$). Setting $\beta = 0$ and $\gamma = 1$ with the dimensionless time going to at least 0.90 should provide a valuable verification check for computer codes.

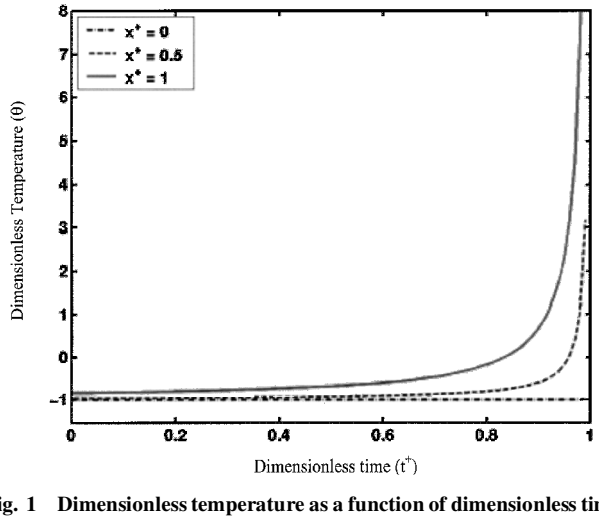

Fig. 1 Dimensionless temperature as a function of dimensionless time for various dimensionless locations, $\beta = 0$ and $\gamma = 1.0$.

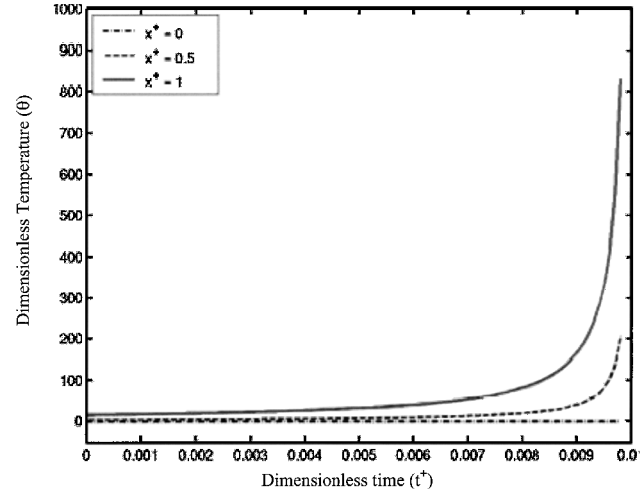

Fig. 2 Dimensionless temperature as a function of dimensionless time for various dimensionless locations, $\beta = 0$ and $\gamma = 0.01$.

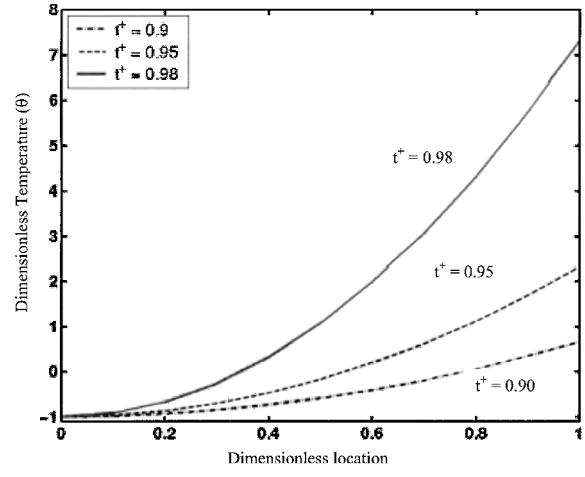

Fig. 3 Dimensionless temperature as a function of dimensionless location for various dimensionless times, $\beta = 0$ and $\gamma = 1.0$.

V. Verification Results

As part of the Accelerated Strategic Computing Initiative program of the Department of Energy, a general framework for solving computational physical models is being developed. A finite element thermal analysis code being implemented in this framework is CALORE. The nonlinear analytical solution developed here is used for verification of CALORE.

We are free to select the thermal properties, time, and constants β and γ in the analytical solution [Eq. (19)] for verification. However, to assess the accuracy of finite element solution, a problem with (spatial) curvature, relative to the order of the basis functions used in the finite element discretization, is needed. As already demonstrated, the nearer the (dimensionless) time is to γ, the more curvature the solution exhibits (Fig. 3). Because linear elements (basis functions) are to be used in the finite element solution, by the selection of the dimensionless time such that it approaches the magnitude of γ, the analytical solution has a curvature that is of higher order than the linear elements. For the verification study, thermal conductivity is taken to have variation described by $k_0 = 1.0$ W/m · K and $k_1 = 1.0$ K^{-1}, whereas volumetric heat capacity is $c = 1.0$ J/m^3 · K. The values of $\beta = 0$ and $\gamma = 0.44$ are selected somewhat arbitrarily. This is because the specific time to evaluate the solution can be chosen such that dimensionless time is near γ. Given the specified constants (β and γ) and values selected for the thermal properties, a time of $t = 0.4$ s gives a dimensionless time $t^+ = 0.4$.

Because CALORE presently solves only three-dimensional problems, we consider a three-dimensional unit cube ($1 \times 1 \times 1$ m^3)

Table 1 Norm values for finite element approximation error in a nonlinear conduction problem while maintaining a constant mesh Fourier number during discritization refinement

Mesh size h, m	$\log_{10}(h)$	L_∞, °C	$\log_{10}(L_\infty)$	L_2, °C	$\log_{10}(L_2)$	H_1, °C/m	$\log_{10}(H_1)$
1/5	−0.70	1.06	0.026	9.12E−01	−0.040	1.07	0.0302
1/10	−1.00	2.68E−01	−0.572	2.07E−01	−0.683	4.46E−01	−0.350
1/20	−1.30	6.65E−02	−1.18	4.99E−02	−1.30	1.51E−01	−0.823
1/40	−1.60	1.72E−02	−1.77	1.28E−02	−1.89	6.54E−02	−1.18
	Slope, p		1.986		2.054		1.368
$\|e\|_m = Ch^p$	Coefficient, $\log(C)$		1.413		1.383		0.992

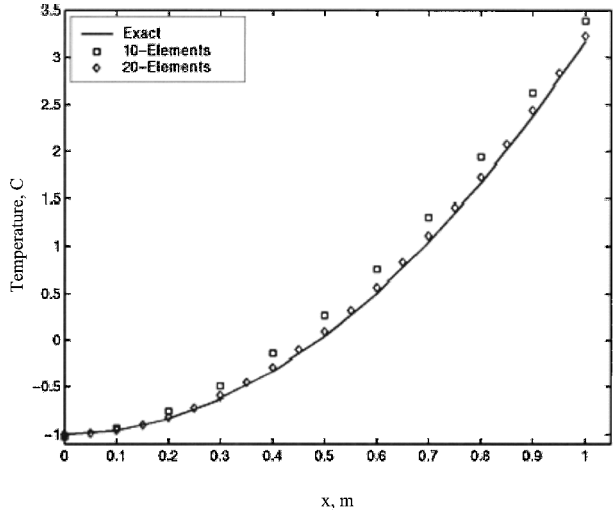

Fig. 4 Comparison of nonlinear analytical solution with a finite element solution.

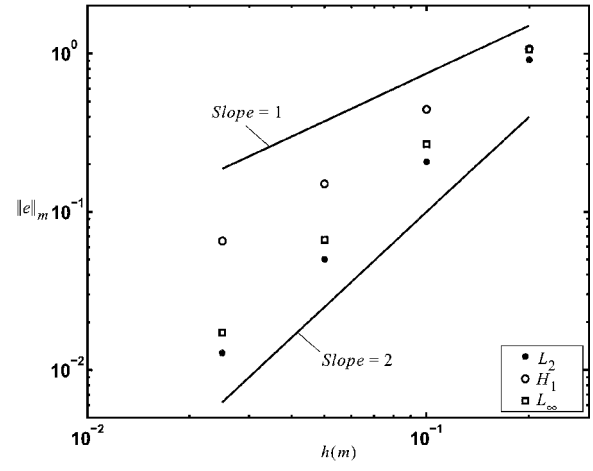

Fig. 5 Error norms for discritization refinement with a variable time step, selected to maintain a constant mesh Fourier number.

with only a single element across the y–z plane to match the one-dimensional analytical solution. The imposed initial condition and boundary conditions for the finite element model are derived from the analytical solution. The initial condition [Eq. (22)] is derived by evaluating the solution at $t = 0$, and the heat flux boundary conditions on the $x = 0$ and 1 face are given in Eqs. (25a) and (25b). Mesh densities $1/h$ along the x direction of 5, 10, 20, and 40 elements are studied. The time step is correspondingly decreased as the mesh is refined; time steps Δt are 0.04, 0.01, 0.0025, and 0.000625 s, for the four mesh densities, respectively. Time steps are selected such that the mesh Fourier

$$Fo_h = (k_0/c)\Delta t \big/ h^2 \tag{32}$$

remains a constant value of 1.0 as the mesh is refined. A backward Euler time integrator is used. Convergence tolerances of $1.0E-10$ are specified for both the Picard iteration for solving the nonlinear problem and for the iterative method used to solve the linear system (matrix) of equations.

The numerical (finite element solution) and exact analytical temperature as a function of position are shown in Fig. 4 for mesh densities of 10 and 20 elements at a time of 0.4 s. The conductivity variation $k(T) = k_0(1 + k_1 T) = 1 + T$, for the selected values of k_0 and k_1. Hence, conductivity varies appreciably in magnitude from 0 to over 4 W/m · K over the spatial domain. The spatial variation of conductivity is identical in form to the temperature distribution shown in Fig. 4. The finite element solution has a maximum error of 8 and 2% for 10 and 20 elements, respectively, which decreases to less than 0.5% with 40 elements. Given this agreement, one has reasonable evidence that there are no significant errors or bugs affecting the accuracy of the finite element solution (for the parts of the code exercised by this solution). To be certain there are no errors, however, we need to study the convergence rate of the error as the discretization is refined.

The finite element solution is an approximation. To complete verification, we must study the nature of the approximate solution and its dependence on the discretization and compare convergence rates for the discretization error with theoretical values. For this purpose, we need to quantify the error[8] in the approximate solution.

Three error norms/seminorms are studied to quantify the difference between the analytical solution T and the approximate finite element solution T^N (Ref. 8). Because this is a transient solution, we shall select a time t at which to evaluate the error. We discuss the interplay between time and space discretizations next. The first norm is based on the maximum error in the spatial domain of the solution ($\Omega = [0, L]$)

$$L_\infty = \|e\|_\infty = \max_{x \in \Omega} |T^N(x,t) - T(x,t)| \tag{33}$$

The second error norm integrates the squared differences in temperature over the domain

$$L_2 = \|e\|_0 = \left(\int_\Omega [T^N(x,t) - T(x,t)]^2 \, \mathrm{d}x \right)^{\frac{1}{2}} \tag{34}$$

which is commonly called the L_2 norm. The third error is a seminorm that involves the first derivative of the solution integrated over the domain

$$H_1 = |e|_1 = \left\{ \int_\Omega \left[\frac{\mathrm{d}T^N(x,t)}{\mathrm{d}x} - \frac{\mathrm{d}T(x,t)}{\mathrm{d}x} \right]^2 \mathrm{d}x \right\}^{\frac{1}{2}} \tag{35}$$

We shall study the convergence of the finite element solution in these error measures.

The error norms as a function of mesh size h are listed in Table 1. The norms were generated for a solution using values of $k_0 = 1.0$ W/m · K, $k_1 = 1.0$ K^{-1}, $c = 1.0$ J/m^3 · K, and $t = 0.4$ s, where $\beta = 0$ and $\gamma = 0.44$. A log plot of the error norms as the mesh size is reduced is shown in Fig. 5. Coefficients from a linear fit to the log of the error norms are listed for each error norm/seminorm under the data in Table 1. As a reference, lines with slope equal to 1 and 2 are shown in Fig. 5.

Norms L_2 and L_∞ are seen to decrease nominally with a slope of 2 as the mesh size decreases; the finite element discretization

Table 2 Norm values for finite element approximation error in a nonlinear conduction problem while maintaining a constant time step ($\Delta t = 0.000005$ s) during discretization refinement

Mesh size h, m	$\log_{10}(h)$	L_∞,°C	$\log_{10}(L_\infty)$	L_2,°C	$\log_{10}(L_2)$	H_1,°C/m	$\log_{10}(H_1)$
1/5	−0.70	3.37E−02	−1.47	1.42E−02	−1.84	4.82E−01	−0.317
1/10	−1.00	8.33E−03	−2.08	3.57E−03	−2.45	2.41E−01	−0.619
1/20	−1.30	2.08E−03	−2.68	9.21E−04	−3.04	1.02E−01	−0.920
1/40	−1.60	5.20E−04	−3.28	2.32E−04	−3.63	6.02E−02	−1.22
	Slope, p		2.005		1.976		1.001
$\|e\|_m = Ch^p$	Coefficient, $\log(C)$		−0.0725		−0.4687		0.3819

scheme is second order in these error norms. The seminorm H_1, which involves the derivative of the solution, decreases with a slope of approximately 1.4. Not surprisingly, error in the derivative of the solution decreases at a lower rate than the error in the solution. To understand whether demonstrated convergence rates are appropriate and the code is correct, the theoretical convergence rates are studied.

The approximate error for a linear finite element solution can be derived[8,9] as

$$\|e\|_m \leq c' h^{s+1-m} \|T\|_{s+1} \tag{36}$$

where c' is a constant (independent of h and T), h is the characteristic length of an element, s is the degree of polynomial in the finite element shape function, and m is the order of the highest derivative appearing in the norm/seminorm expression. In Eq. (36), we have assumed the analytical solution T is sufficiently smooth, meaning the analytical solution has bound derivatives up to (at least) $s+1$. Linear elements are used for these analysis, that is, $s=1$, and the analytical solution has bound second derivatives $(s+1)$. Substituting for s and combining c' with the norm of the analytical solution in Eq. (36) gives

$$\|e\|_m \leq Ch^p \tag{37}$$

The rate of convergence is $p=(2-m)$ and C is a constant with respect to h, which can depend on the smoothness of the analytical solution. The theoretical basis for this result is a linear analysis. Although the problem addressed here is nonlinear, the linear analysis provides, at least, a limiting case as the nonlinear solution approaches the linear case.

Theoretical dependence of the approximation error, assuming a linear problem, is given in Eq. (37). The L_2 norm, $m=0$, should converge with a slope of 2, that is, second-order accuracy. Although the problem is nonlinear, the results for the L_2 norm in Table 1 and Fig. 5 demonstrate the theoretical accuracy. The seminorm H_1, $m=1$, should converge with a slope of 1 and demonstrate first-order accuracy. We achieve a slightly higher convergence rate of 1.4. Given that the L_2 norm follows the theoretical rate, we would expect the H_1 seminorm to follow accordingly, but it does not. We investigate this outcome next. Although the theory does not apply to the local nature of the L_∞ norm, its demonstrated convergence rate is second order.

The approach taken to study the dependence on discretization for this transient problem is to refine the spatial and time discretization simultaneously such that the mesh Fourier number [Eq. (32)] remains constant. One can show the local truncation error for a linear problem depends on the mesh Fourier number. Furthermore, we have demonstrated the theoretical convergence rate (first order) for the H_1 seminorm while maintaining a constant mesh Fourier number for a linear problem (using the same computer code). In the nonlinear case, this may not hold. To investigate the dependence of our earlier results (generated while maintaining a constant mesh Fourier number) on the selected time step and the general approach, we used a fixed time step while refining the spatial discretization. We repeated the process while refining the time step until the error norms reached the asymptotic region. The grid convergence results as a function of selected time step are shown in Fig. 6 and listed in Table 2 for the time step for which the norms are in the asymptotic region.

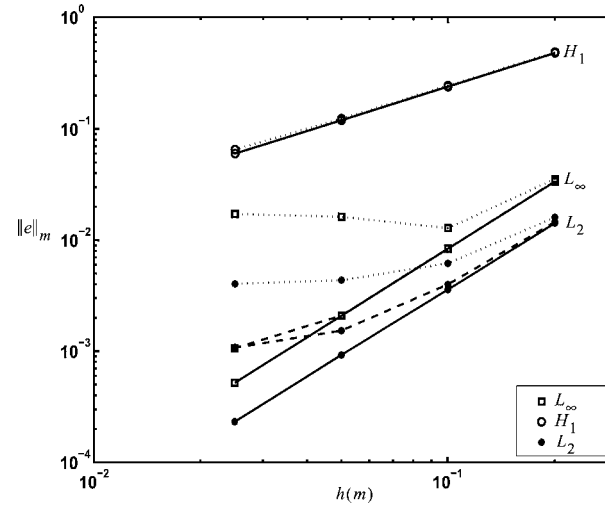

Fig. 6 Error norm for discretization refinement with a fixed time step.

The demonstrated convergence rate (Table 2 and Fig 6) for the seminorm H_1 using a fixed time step while refining spatially agrees with the theoretical value; convergence is first order. Furthermore, notice that the seminorm is fairly insensitive to the selected time step. The L_2 and L_∞ norms require the time step to be decreased nearly two orders of magnitude (compared to the smallest time step used while maintaining a constant mesh Fourier number) to reach the asymptotic region. However, the convergence rate for L_2 and L_∞ norms is nominally the same as that observed while maintaining the mesh Fourier number constant, both norms are second order.

For the nonlinear case, these data demonstrate that maintaining a constant mesh Fourier number will result in an expected convergence rates for the L_2 and L_∞ norms, but gives an unexpected convergence rate for the seminorm H_1. Maintaining the time step constant while refining the spatial discretization gives the expected convergence rate for all norms. The seminorm H_1 is insensitive to the magnitude of the time step, but the L_2 and L_∞ norms require the time step to be reduced significantly to reach the asymptotic region. Convergence rates based on the linear theory were realized for the nonlinear verification problem.

Finally, with the demonstrated accuracy and convergence rates, we have documented evidence that the finite element code is correctly solving the nonlinear thermal diffusion equation.

VI. Conclusions

An analytical solution to the equation for nonlinear thermal diffusion with thermal conductivity varying linearly with temperature and all other thermal properties constant has been presented. Because of the dependence of the boundary and initial conditions (which are generated from the solution itself) on location and time, the solution has limited application for physically based problems. The solution methodology and analytical techniques to derive the solution are potentially useful for solving other related problems. Use of the analytical solution to verify a finite element numerical code for solving nonlinear heat conduction was presented. Accuracy of the numerical solution and the expected rate of convergence of the discretization error were demonstrated.

Acknowledgments

Sandia National Laboratories is a multiprogram laboratory operated by Sandia Corp., a Lockheed Martin Co., for the U.S. Department of Energy under Contract DE-AC04-94AL85000. Insightful comments and suggestions from T. Voth, B. Blackwell, and J. Stewart, all at Sandia National Laboratories, were helpful in compiling and interpreting the verification results.

References

[1]Sturm, J. C. F., and Liouville, J., *Journal de Mathematique*, Vols. 1–3, 1836–1838.

[2]Beck, J. V., Cole K. D., Haji-Sheikh, A., and Litkouhi, B., *Heat Conduction Using Greens Functions*, Hemisphere, Washington, DC, 1992, Chap. 3.

[3]Ozisik, M. N., *Heat Conduction*, Wiley, New York, 1980, Chap. 6.

[4]Becker, M., "Nonlinear Transient Heat Conduction Using Similarity Groups," *Journal of Heat Transfer*, Vol. 122, 2000, pp. 33–39.

[5]Incropera, F., and DeWitt, D., *Introduction to Heat Transfer*, Wiley, New York, 1990, Appendix A.

[6]Roach, P. J., "Verification and Validation in Computational Science and Engineering," Hermosa, Albuquerque, NM, 1998, Chaps. 3–8.

[7]"Guide for the Verification and Validation of Computational Fluid Dynamics Simulation," AIAA-G-077-1998, 1998.

[8]Hughes, T. J. R., *The Finite Element Method*, Prentice, New York, 1987, Chap. 4.

[9]Stewart, J. R., and Hughes, T. J. R., "A Tutorial in Elementary Finite Element Error Analysis: A Systematic Presentation of A Priori and A Posteriori Error Estimates," *Computational Methods in Applied Mechanical Engineering*, Vol. 158, 1998, pp. 1–22.